Biochemistry

 Volume 19, Number 15 July 22, 1980

Ligand Interactions with Membrane-Bound Porcine Atrial Muscarinic Receptor(s)†

Michael I. Schimerlik* and Robert P. Searles

ABSTRACT: Ligand interactions with the membrane-bound muscarinic acetylcholine receptor in porcine atria are characterized by using [^{3}H]quinuclidinyl benzilate [Yamamura, H. I., & Snyder, S. H. (1974) *Proc. Natl. Acad. Sci. U.S.A. 71*, 1725–1729] as a probe for the receptor. Antagonists and local anesthetics appear to displace quinuclidinyl benzilate from a single population of high-affinity sites while agonists appear to interact with two noninterconvertible subpopulations of quinuclidinyl benzilate binding sites. The simplest mechanism that appeared to be consistent with both kinetic and thermodynamic studies of [^{3}H]QNB binding to the receptor required two steps. The first step, in rapid preequilibrium (K = 1.8 × 10^{-9} M), was followed by a slow ligand-induced conformational change (k_1 = 5.5 × 10^{-3} s^{-1}; k_{-1} = 3.3 × 10^{-4} s^{-1}) of the receptor–QNB complex. The overall dissociation constant calculated from the kinetic data (1.09 × 10^{-10} M) was in good agreement with that determined from equilibrium measurements (K_{ov} = 1.22 × 10^{-10} M). The complex behavior of the dissociation rate constant for [^{3}H]quinuclidinyl benzilate in the presence of competing ligands may indicate that at high concentrations these ligands either bind to a second low-affinity site(s) on the protein, altering the properties of the high-affinity site, or they nonspecifically alter the properties of the membrane, creating a second population of quinuclidinyl benzilate–receptor complexes that dissociate with an observed rate constant equal to ~3 × 10^{-5} s^{-1}.

To date, most studies on the membrane-bound mAcChR[1] have been done by using either rat heart (Cavey et al., 1977; Fields et al., 1978), rat brain (Birdsall & Hulme, 1976; Hulme et al., 1978; Birdsall et al., 1978), neural cell lines (Strange et al., 1978; Burgermeister et al., 1978), or developing chick heart (Galper et al., 1977). Using the affinity alkylating agent PrBCM as well as direct binding studies with labeled agonists and antagonists, Hulme et al. (1978) and Birdsall et al. (1978) have shown that brain mAcChR appears to be homogeneous with respect to interactions with antagonists; however, the preparation shows at least two classes of noninteracting sites with respect to agonist interactions. Physiological experiments in isolated rabbit heart (Sharma & Banerjee, 1978) have also demonstrated the existence of both pre- and postsynaptic mAcChR's in that destruction of sympathetic nerve endings by injection of 6-hydroxydopamine eliminated ~40% of the toal number of mAcChR's without altering the ligand binding properties of the remaining 60%.

The properties of rat heart mAcChR's have been studied by using a radiolabeled derivative of the potent muscarinic antagonist QNB (Yamamura & Snyder, 1974). The data from different laboratories are conflicting with regard to the mechanism of QNB–mAcChR interaction. Fields et al. (1978) reported that the interaction is a simple bimolecular association reaction. However, Cavey et al. (1977) have inferred an isomerization following binding of QNB to the receptor on the basis of an observed association rate at least 1 order of magnitude lower than that expected for a diffusion-controlled reaction. In the developing chick hearts, Galper et al. (1977) observed two exponentials for QNB binding, postulating a two-step mechanism. In the latter case, the slow kinetic phase was not treated quantitatively to determine all the rate and equilibrium constants in the proposed mechanism. Furthermore, the above systems suffer from the disadvantage that large quantities of membrane-bound mAcChR cannot be easily prepared so that the eventual purification of the protein from these sources may prove difficult.

The purpose of this paper is twofold. First, it presents the characterization of the membrane-bound mAcChR from pig atria with respect to interactions with agonists, antagonists, and local anesthetics. Since large quantities of atrial tissue are readily available and the porcine heart and circulatory system in many respects resembles that of man (Detwiler, 1966), this system may provide enough material for future studies on the membrane-bound mAcChR and eventually the solubilized purified protein. Second, kinetic studies of the interaction of [^{3}H]QNB with the mAcChR permitted the quantitative treatment of a mechanism in which QNB binds

† From the Department of Biochemistry and Biophysics, Oregon State University, Corvallis, Oregon 97331. *Received February 21, 1980.* Supported by grants from the Medical Research Foundation of Oregon, The Oregon Heart Association, and National Institutes of Health Biomedical Research Support Grant RR 07079.

[1] Abbreviations used: mAcChR, muscarinic acetylcholine receptor; QNB, quinuclidinyl benzilate; [^{3}H]QNB, tritium-labeled quinuclidinyl benzilate; EDTA, ethylenediaminetetraacetic acid; PMSF, phenylmethanesulfonyl fluoride; PrBCM, propylbenzilylcholine mustard; BSA, bovine serum albumin.

0006-2960/80/0419-3407$01.00/0

in rapid preequilibrium with the mAcChR, followed by a slow conformational change of the mAcChR–QNB complex.

Materials and Methods

Atrial microsomes were prepared from pig hearts removed immediately after slaughter. Typically, 100 g of atria was washed clean of blood, cut into small pieces, and added to ice-cold buffer (50 mM sodium phosphate, 0.02% w/v sodium azide, 1 mM EDTA, and 1 mM PMSF, pH 7.4; 8 mL of buffer/g of tissue). The tissue suspension was then homogenized under argon at 4 °C (twice, for 1-min each) by using a Polytron homogenizer equipped with the PT35ST probe. The crude homogenate was centrifuged at 600*g* for 10 min to remove cellular debris. The supernatant was filtered through cheesecloth and then centrifuged for 1 h at 70000*g*. The buff-colored layer around the pellet was gently resuspended in the above buffer with a spatula and centrifuged as before. mAcChR concentration was quantitated in terms of QNB sites as described by Yamamura & Snyder (1974) while protein was assayed by the method of Lowry et al. (1951) with crystalline BSA as a standard. The final microsomal suspension generally had a specific activity of ~700–800 pmol of QNB sites/g of protein and yielded a five- to sevenfold purification (25–35% recovery) over that of the crude homogenate fraction. The microsomal preparation was either used at once or divided into 3-mL aliquots and stored frozen at −80 °C. Control experiments showed that frozen and thawed preparations had the same properties as nonfrozen preparations; therefore, they were used interchangeably in both kinetic and equilibrium experiments.

[^{3}H]QNB (29.4 Ci/mmol), purchased from New England Nuclear, cochromatographed with a nonlabeled standard (the generous gift of Dr. W. E. Scott, Hoffman-La Roche Inc.) on Merck silica gel 60 plates in acetone–methanol–diethanolamine (10:10:0.3; R_f = 0.34) and chloroform–methanol (9:1; R_f = 0.10) solvent systems with over 98% of the radioactivity found in the QNB spot. Acetylcholine, eserine, carbamylcholine, atropine, l-hyoscyamine, choline, scopolamine, tetracaine, and dibucaine were purchased from Sigma Chemical Co. Pilocarpine and oxotremorine were purchased from Aldrich Chemical Co., and dibucaine, procainamide, lidocaine, and quinidine were supplied by Pfaltz & Bauer. α-Bungarotoxin, purified by the method of Clarke et al. (1972), was the generous gift of Professor M. A. Raftery.

Equilibrium titrations were performed as described by Fields et al. (1978). After equilibrium was attained, an aliquot was removed for scintillation counting (Triton–toluene scintillation fluid; Beckman Model L53133P scintillation counter) to determine the total [^{3}H]QNB concentration. [^{3}H]QNB bound was determined by counting the label remaining on the disk after filtration and washing 3 times with 5-mL aliquots of cold buffer. Free ligand was then calculated from total minus bound [^{3}H]QNB. Nonspecifically bound [^{3}H]QNB was determined in a duplicate experiment done in the presence of 1.0 μM atropine. At [^{3}H]QNB up to 1 nM less than 5% of the label bound was nonspecific in nature. In kinetic experiments the GF/B glass fiber disks were washed once with 7 mL of cold buffer.

The rate constant for [^{3}H]QNB dissociation from the membrane-bound mAcChR was measured either by 100-fold dilution of the mAcChR–QNB complex (final concentration of [^{3}H]QNB and QNB binding sites was 29 and 30 pM, respectively) into atropine (concentration range 10 nM–100 μM) or by direct addition of atropine (or other ligands; see below) to a solution in which [^{3}H]QNB and membrane vesicles had been equilibrated. Similar rate constants for dissociation were observed when the competing ligand was added to the membrane suspension 3 min or 1 h after the [^{3}H]QNB. [^{3}H]QNB bound at equilibrium was determined when there was no further change in counts per minute bound over an interval of 12 h. Control experiments showed that the mAcChR–[^{3}H]QNB complex was stable at room temperature for at least 72 h. The total amplitudes of the displacement corresponded to that predicted from the law of mass action calculated by using the equilibrium dissociation constants determined experimentally.

All experiments were done by using the previously described buffer except the acetylcholine titration for which the pH was adjusted to 6.9 and 10 μM eserine was added. Control experiments showed that this concentration of eserine did not interfere with [^{3}H]QNB binding to the microsomal preparation.

Data Evaluation

Equilibrium titration curves measuring [^{3}H]QNB displacment were analyzed in two ways. Dissociation constants of the ligands that appeared to displace [^{3}H]QNB in a competitive manner (antagonists; local anesthetics) were determined by a weighted least-squares fit to the $\bar{j}$ function (eq 1; Figure 3) as described by Best-Belpomme & Dessen (1973). [I_0] and [R_0] equal the total inhibitor and QNB site concentrations while $\overline{RQ}$ and $\overline{RQ}_0$ are the fractional saturation of QNB sites in the presence of inhibitor at concentration [I_0] and in the absence of inhibitor. [Q] and [RQ] are the concentrations of free and specifically bound [^{3}H]QNB at each inhibitor concentration and K_i and K are the dissociation constants of the inhibitor and QNB. Thus, a plot of $\bar{j}$ vs. [Q]/[RQ] is linear, going through the origin, permitting calculation of K_i from the slope once K is determined. Data for agonists were fitted to a model (described in the Appendix) that allowed for competition occurring at two classes of agonist site that are homogeneous with respect to interactions with QNB. The reasoning behind this assumption is given in the text.

$$\frac{[I_0]}{[R_0](1 - \overline{RQ}/\overline{RQ}_0)} - 1 = \bar{j} = \frac{[Q]}{[RQ]}\frac{K_i}{K} \qquad (1)$$

Kinetic data (see Figure 2) were analyzed by a least-squares fit to eq 2 where τ^{-1} is the relaxation time, $(cpm)_t$ is the radioactivity bound at time t, $(cpm)_\infty$ is the radioactivity bound at equilibrium (4–5 h for these experiments), and $(cpm)_{NS}$ is the nonspecifically bound [^{3}H]QNB. Control experiments showed that nonspecific binding (due mostly to binding to the GF/B filters) equilibrated rapidly compared to [^{3}H]QNB association with the mAcChR. Therefore, it is an additive constant to both terms in the numerator of the fraction in eq 2 and cancels.

$$\ln \frac{(cpm)_\infty - (cpm)_t}{(cpm)_\infty - (cpm)_{NS}} = -t\tau^{-1} \qquad (2)$$

The fit of the data in Figure 3 to eq 5 in the text was done by the method of weighted least squares where weighting factors were renormalized according to Bevington (1969). k_{-1} was estimated from an extrapolation of a plot of τ^{-1} vs. [^{3}H]QNB concentration to zero, and k_1 and K were then calculated from the weighted semireciprocal fit (Figure 3, insert).

When the kinetics of [^{3}H]QNB dissociation from the mAcChR were measured under conditions of atropine concentrations greater than 100 nM (see the text), two exponentials with relaxation times differing by a factor of ~10 were observed. These data were evaluated by using least-

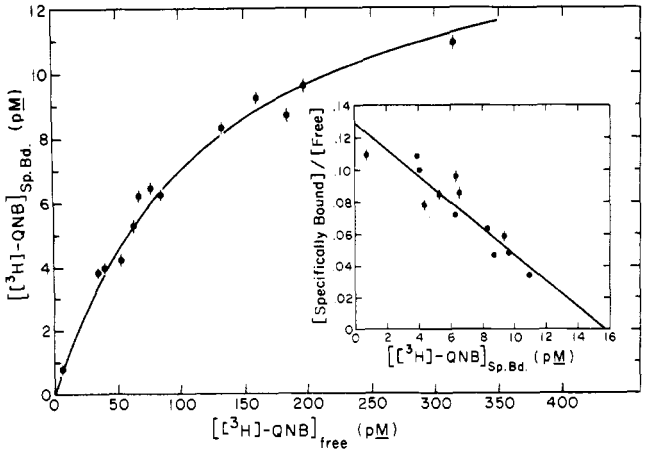

FIGURE 1: [^{3}H]QNB binding to porcine atrial microsomes. Atrial microsomes, 15 pM in [^{3}H]QNB sites in a total volume of 12 mL, were equilibrated for 1 h at 25 °C with varying concentrations of [^{3}H]QNB. After removal of duplicate aliquots for measurement of the total [^{3}H]QNB concentration, 10-mL samples were filtered and washed as described under Materials and Methods. After correction for nonspecifically bound [^{3}H]QNB (see Materials and Methods), data were plotted in the form of a Scatchard plot (insert). Data points are the average of duplicate samples. Linear least-squares analysis gave a dissociation constant, calculated from the reciprocal of the slope, equal to $(1.24 \pm 0.10) \times 10^{-10}$ M and the total number of QNB sites, from the abscissa, equal to 15.7 ± 0.5 pM. The curve drawn through the data points was computed from the law of mass action by using the calculated dissociation constant and experimentally determined free [^{3}H]QNB concentration.

squares methods (Bevington, 1969) by first fitting the slow phase after the more rapid phase had decayed. After subtraction of the slow phase, the fast phase was evaluated.

Results

QNB Interactions with the mAcChR. mAcChR interactions with QNB were studied quantitatively using both equilibrium and kinetic measurements. Figure 1 shows a Scatchard plot (Scatchard, 1949) of [^{3}H]QNB binding to porcine atrial microsomes. From the slope of the regression line, an overall dissociation constant of $(1.24 \pm 0.10) \times 10^{-10}$ M was calculated. The weighted average [$(1.22 \pm 0.12) \times 10^{-10}$ M] of three such experiments was used in eq 1 for all further calculations.

The kinetic studies measuring the rate of QNB association were performed under pseudo-first-order conditions ([[^{3}H]-QNB]$_0 \gg$ [QNB sites]$_0$). As can be seen in Figure 2, only a single relaxation time was observed to over 90% of completion of the reaction. The data (insert, Figure 2) plotted in semilogarithmic form as ln (percent QNB sites remaining) vs. time extrapolates to an ordinate intercept of 97 ± 5%, indicating that all of the specifically bound [^{3}H]QNB can be accounted for by the single kinetic phase. When τ^{-1} was replotted vs. [^{3}H]QNB concentration (Figure 3), it was nonlinear, leveling off at higher QNB concentrations. A simple bimolecular association reaction should show a linear dependence of τ^{-1} on QNB concentration and can therefore be discarded (also see Discussion). The simplest mechanism consistent with these data in Figure 3 is

$$R + Q \overset{K}{\rightleftharpoons} RQ \underset{k_{-1}}{\overset{k_1}{\rightleftharpoons}} RQ' \qquad (3)$$

where Q and R are free mAcChR and [^{3}H]QNB, respectively. The QNB is considered to be in rapid equilibrium with the mAcChR complex RQ with $K = [Q][R]/[RQ]$. After the binding of QNB, a slow conformational change occurs from RQ to RQ′ with first-order rate constant k_1 in the forward

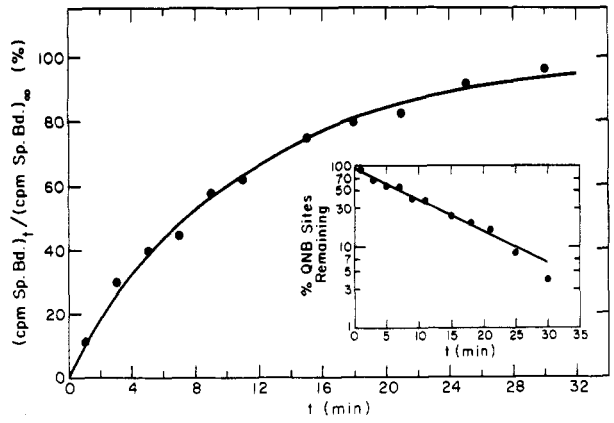

FIGURE 2: Time course for [^{3}H]QNB association. [^{3}H]QNB, final concentration 304 pM, was added to the membrane-bound mAcChR, final concentration 30 pM in QNB sites (0.11 mg of protein/mL), at time zero. Aliquots were removed and filtered at the indicated times, and the data were corrected for nonspecific binding as described under Materials and Methods. The data were evaluated (insert) by a least-squares fit to the semilogarithmic plot to give $k_{obsd} = (1.66 \pm 0.10) \times 10^{-3}$ s^{-1} and an ordinate intercept of 97 ± 5%. The curve drawn through the data points is the theoretical curve calculated for a single exponential by using the above values.

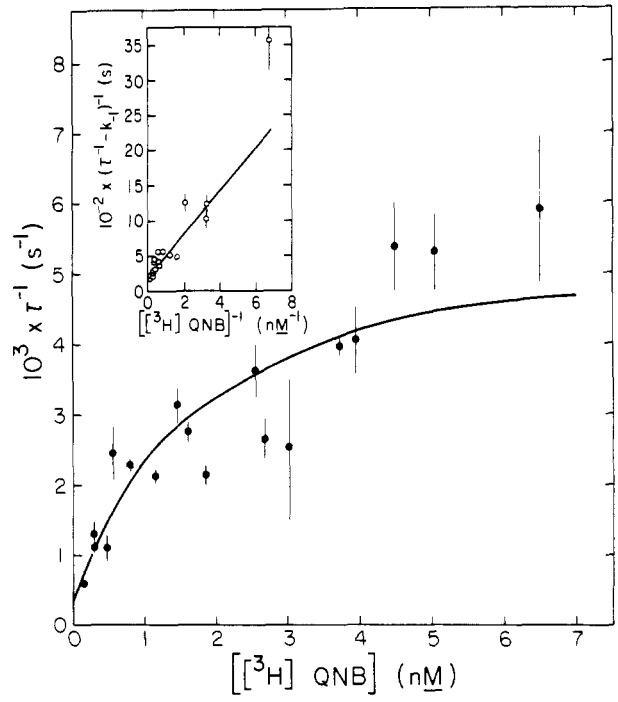

FIGURE 3: Dependence of τ^{-1} on [^{3}H]QNB concentration. The curve through the data points was calculated from eq 4 in the text by using the values of $k_1 = 5.5 \times 10^{-3}$ s^{-1}, $k_{-1} = 3.3 \times 10^{-4}$ s^{-1}, and $K = 1.8 \times 10^{-9}$ M. The insert is the weighted least-squares fit to eq 5 which allowed calculation of k_1 [$(5.5 \pm 0.3) \times 10^{-3}$ s^{-1}] and K [$(1.80 \pm 0.12) \times 10^{-9}$ M] by using the above estimate of k_{-1}.

direction. The bound radioactivity arises exclusively from the RQ′ complex. In the case where the first step is unobservably fast, a single relaxation time is predicted for mechanism 3, given by eq 4; otherwise, two relaxation times should be observed (Quast et al., 1974):

$$\tau^{-1} = k_{-1} + k_1[Q]/([Q] + K) \qquad (4)$$

The constants in eq 4 were computed by a weighted least-squares fit to the linearized form of eq 4 (see Data Evaluation):

$$(\tau^{-1} - k_{-1})^{-1} = (K/k_1)(1/[Q]) + 1/k_1 \qquad (5)$$

The calculated values for the respective rate and equilibrium

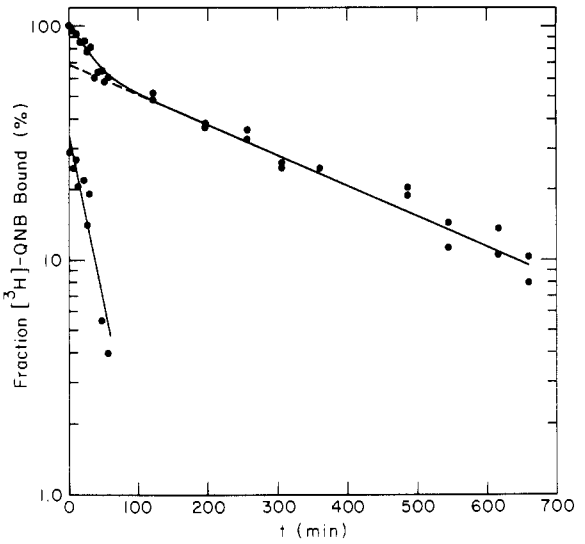

FIGURE 4: Time course for QNB dissociation. Atropine (100 nM) was added at time zero to a suspension of membrane-bound mAcChR (0.3 nM in QNB sites) plus 2 nM [^{3}H]QNB, and the dissociation reaction was followed as described under Materials and Methods. Data were evaluated by a least-squares fit to the slow exponential using data obtained after t = 200 min [$\delta A_2/\delta A_t$ = 68 ± 7%; τ_2^{-1} = (4.95 ± 0.27) × 10^{-5} s^{-1}]. The fast exponential was then evaluated after subtraction of the slow phase [$\delta A_1/\delta A_t$ = 32 ± 8%; τ_1^{-1} = (5.38 ± 1.43) × 10^{-4} s^{-1}; lower line). It should be noted that three of the data points could not be used to evaluate the fast phase since they gave negative or zero values when the slow phase was subtracted. The curve through the data points is the calculated curve using the above experimentally determined values.

constants were as follows: k_1 = (5.5 ± 0.3) × 10^{-3} s^{-1}, k_{-1} = 3.3 × 10^{-4} s^{-1}, and K = (1.80 ± 0.12) × 10^{-9} M. Under these conditions $K_1 = k_{-1}/k_1 \ll 1$ and K_{ov} = [R][Q]/([RQ] + [RQ']) was approximately equal to KK_1. The calculated value for K_{ov} = (1.09 ± 0.10) × 10^{-10} M is in excellent agreement with the value computed from the Scatchard plot, indicating the consistency between the kinetic and thermodynamic measurements.

When an attempt was made to directly determine the rate constant for dissociation of [^{3}H]QNB from the mAcChR, complex kinetic behavior was observed. At high concentrations of atropine (100 μM), a single exponential (τ_2^{-1}) was observed having a relaxation time equal to (3.3 ± 0.1) × 10^{-5} s^{-1}, a factor of ~10-fold lower than that predicted from the data in Figure 3. At lower atropine concentrations (0.1 μM; see Figure 4), a second faster phase appeared (τ_1^{-1} = (5.4 ± 0.2) × 10^{-4} s^{-1}; $\delta A_1/\delta A_t$ ~ 30%; Figure 4) whose relaxation time corresponded to that predicted by the fit of the data in Figure 3 to the mechanism in eq 3. At still lower atropine concentrations (10–100 nM), only a single fast phase was observed (τ_1^{-1} varied between 1 × 10^{-4} and 9 × 10^{-4} s^{-1}) for several different preparations. Over the range of atropine concentrations studied (10 nM–100 μM; see Table I), the amplitude completely shifted from the slow to the fast phase; however, within a factor of 4, the observed rate of dissociation of [^{3}H]QNB remained constant (e.g., ~5 × 10^{-4} s^{-1}). Similar results were found when oxotremarine or nonlabeled QNB were used as competing ligands. The dependence of the observed data constants and amplitudes on ligand concentration are summarized in Table I. These data show that although the relative amplitude of the two kinetic phases depended on ligand concentration, the observed rate constants for dissociation did not vary significantly either with the structure of the competing ligand or with the concentration of [^{3}H]QNB (0.02–2 nM).

Table I: Effect of Competing Ligand on [^{3}H]QNB Dissociation[a]

ligand	concn (nM)	$\delta A_1/\delta A_t$ (%)	τ_1^{-1} × 10^4 (s^{-1})	$\delta A_2/\delta A_t$ (%)	τ_2^{-1} × 10^5 (s^{-1})
atropine	10	100 ± 8	9.2 ± 0.5		
	34	100 ± 5	1.0 ± 0.1		
	100	32 ± 8	5.4 ± 1.4	68 ± 7	5.0 ± 0.3
	10 000	23 ± 4	7.0 ± 0.9	77 ± 4	3.3 ± 0.1
	30 000			100 ± 7	9.1 ± 0.4
	100 000			100 ± 1	3.3 ± 0.1
oxotremorine	26 000	29 ± 6	9.2 ± 1.3	71 ± 6	2.5 ± 0.4
	48 000			100 ± 5	7.0 ± 0.3
QNB	8	46 ± 8	3.0 ± 0.7	54 ± 5	4.6 ± 0.4
	40	34 ± 7	5.0 ± 0.8	66 ± 6	4.2 ± 0.3
	1 000	10 ± 2	3.5 ± 1.0	90 ± 3	3.3 ± 0.2
	100 000			100 ± 5	3.5 ± 0.1

[a] Similar results for $\delta A_{1,2}/\delta A_t$ and $k_{1,2}$ were found regardless of whether the competing ligand was added directly to the equilibrium mixture of mAcChR plus [^{3}H]QNB or whether the mixture was diluted 100-fold into competing ligand.

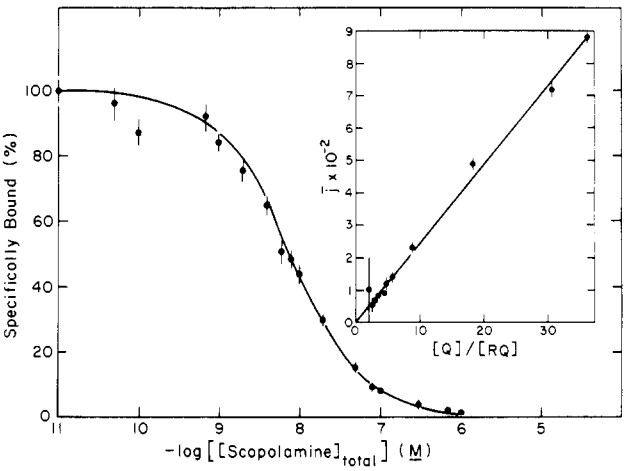

FIGURE 5: Scopolamine titration of specifically bound [^{3}H]QNB. The scopolamine concentration was varied at constant concentrations of mAcChR (122 pM in QNB sites) and [^{3}H]QNB (174 pM). The data points represent the average of three determinations. Procedures are given under Materials and Methods. The data were evaluated by a weighted least-squares fit to the $\bar{j}$ function (insert; see Data Evaluation) to give a value of (2.94 ± 0.05) × 10^{-9} M for the dissociation constant of this ligand. The curve through the data points was calculated from the law of mass action by using 1.22 × 10^{-10} M as the dissociation constant for QNB, the above value for scopolamine, and the experimentally determined concentrations of free [^{3}H]QNB at each data point.

[^{3}H]QNB Displacement by Antagonists and Local Anesthetics. Antagonists and local anesthetics appeared to displace [^{3}H]QNB from the mAcChR in a competitive manner consistent with the law of mass action. A typical antagonist (scopolamine) titration curve is shown in Figure 5. The data were fitted by using the $\bar{j}$ function (Figure 5, insert) and the normalized titration curve calculated from the law of mass action by using the dissociation constants for scopolamine and QNB and the experimentally determined free [^{3}H]QNB concentration. Dissociation constants for both local anesthetics and antagonists are summarized in Table II.

[^{3}H]QNB Displacement by Agonists. A typical agonist (carbamylcholine) titration is shown in Figure 6. Although agonists displaced [^{3}H]QNB from the receptor, the titration curves clearly did not follow the law of mass action for a homogeneous population of sites. The simplest model consistent with both the data and the physiological evidence for pre- and postsynaptic mAcChR's in the heart was to assume that the single population of QNB sites contains two nonin-

Table II: Equilibrium Dissociation Constants for Muscarinic Ligands[a]

classification	compd	F_1	K_1 (M)	F_2	K_2 (M)
antagonists	quinuclidinyl benzilate	1.0	$(1.22 \pm 0.12) \times 10^{-10}$		
	atropine	1.0	$(1.00 \pm 0.05) \times 10^{-9}$		
	l-hyoscyamine	1.0	$(2.8 \pm 0.7) \times 10^{-10}$		
	scopolamine	1.0	$(2.94 \pm 0.05) \times 10^{-9}$		
	choline	1.0	$(5.0 \pm 0.5) \times 10^{-3}$		
agonists	acetylcholine[b]	0.35	1.0×10^{-8}	0.65	6.0×10^{-6}
	oxotremorine	0.35	1.0×10^{-7}	0.65	2.2×10^{-6}
	carbamylcholine	0.35	2×10^{-7}	0.65	7.0×10^{-5}
	pilocarpine	0.20	2.2×10^{-7}	0.80	2.0×10^{-5}
local anesthetics	tetracaine	1.0	$(2.9 \pm 0.4) \times 10^{-5}$		
	lidocaine	1.0	$(7.9 \pm 0.1) \times 10^{-5}$		
	dibucaine	1.0	$(1.5 \pm 0.3) \times 10^{-4}$		
	quinidine	1.0	$(5.4 \pm 0.1) \times 10^{-6}$		
	procainamide	1.0	$(8.2 \pm 0.5) \times 10^{-5}$		
α-bungarotoxin	c	c	c	c	c

[a] pH 7.4 in the previously described buffer. [b] In the presence of 10 μM eserine to inhibit the esterase; control experiments indicated that eserine did not displace [^{3}H]QNB, pH 6.9, to slow base-catalyzed hydrolysis. [c] α-Bungarotoxin (specific for nicotinic acetylcholine receptors; 65 nm) has no effect.

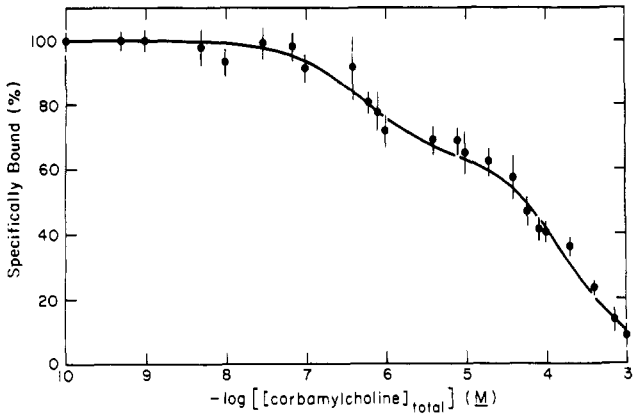

FIGURE 6: Carbamylcholine titration of specifically bound [^{3}H]QNB. Carbamylcholine concentration was varied at constant concentrations of mAcChR (132 pM) and [^{3}H]QNB (240 pM). The data points are an average of three determinations. The curve was calculated from eq A5–A7 (see the Appendix) by using the parameters $K = 1.22 \times 10^{-10}$ M, $F_1 = 0.35$, $K_1 = 2.0 \times 10^{-7}$ M, $F_2 = 0.65$, and $K_2 = 7.0 \times 10^{-5}$ M and the experimentally determined concentrations of free [^{3}H]QNB (see Materials and Methods). Since there was no displacement of [^{3}H]QNB at [carbamylcholine] $< 10^{-7}$ M $\gg$ 10[QNB sites], the concentration of free carbamylcholine was essentially equal to the total ligand concentration.

teracting subpopulations of agonist sites. The data were then fit by an iterative method where the fraction of high- and low-affinity sites (F_1 and F_2) and their respective dissociation constants K_1 and K_2 were varied until an adequate fit was obtained (see the Appendix).

Discussion

The kinetic studies reported here indicate that QNB induces a slow conformational change in the membrane-bound mAcChR from porcine atria. This conformational change results in an order of magnitude increase in affinity for QNB ($K_{ov} = 1.1 \times 10^{-10}$ M) compared to that found in the precomplex ($K = 1.8 \times 10^{-9}$ M). Since there was significant variability in the data in Figure 3, it was also possible to fit the plot of τ^{-1} vs. [[^{3}H]QNB] to a straight line which would be predicted for a simple bimolecular association reaction (R + Q $\rightleftharpoons$ (k_1, k_{-1}) RQ). This data fit yields values of $k_1 = 7.7 \times 10^5$ M^{-1} s^{-1}, $k_{-1} = 1.2 \times 10^{-3}$ s^{-1}, and $K_d = k_{-1}/k_1 = 1.6 \times 10^{-9}$ M. The calculated value of k_1 from this fit is at least 1 order of magnitude too low for a diffusion-controlled bimolecular association [the rate constant for acetylcholine binding to the nicotinic receptor was found to be at least 10^7 M^{-1} s^{-1} (Bonner et al., 1976)], and the value for the K_d was 1 order of magnitude higher than that found in the evaluation of the thermodynamic data (Figure 1). Therefore, the kinetic data in Figure 3 appear to be inconsistent with the simple bimolecular association of QNB with the mAcChR. These data are also inconsistent with a mechanism in which two slowly equilibrating receptor forms are present, only one of which binds QNB (eq 6). This mechanism predicts that the

$$R' \underset{k_{-1}}{\overset{k_1}{\rightleftharpoons}} R + Q \overset{K}{\rightleftharpoons} RQ \qquad (6)$$

observed relaxation rate should decrease as QNB concentration is increased (Hammes & Wu, 1974).

The two-state model (ligand binding steps are fast compared to isomerization steps) in which QNB acts as an allosteric effector shifting the equilibrium from the low- to the high-affinity form of mAcChR can also yield a hyperbolic dependence of τ^{-1} on QNB concentration (Janin, 1973). The prediction of that mechanism is that the dissociation of QNB from the high-affinity form should occur rapidly at high concentrations of competitive inhibitor. The slow rate of [^{3}H]QNB dissociation from the final high-affinity form, however, indicates that [^{3}H]QNB was not dissociating by the rapidly equilibrating step predicted by this mechanism but by a reversal of the mechanism shown in eq 3. Therefore, the two-state mechanism in which QNB acts as an allosteric effector shifting a preexisting equilibrium from the low- to high-affinity state is also inconsistent with the data.

The observation of two exponentials in the kinetics of [^{3}H]QNB dissociation is at variance with previous studies using whole rat heart homogenates (Fields et al., 1978) or membrane preparations (Cavey et al., 1977); however, biphasic kinetics have been observed by using developing chick heart (Galper et al., 1977) or neural cell line NIE-115 (Burgermeister et al., 1978). In the latter two cases, though, the dependence of the relative amplitudes of the two phases on the concentration of competing ligand were not measured; thus, a further comparison cannot be made at this time. The observation of two exponentials is at variance with the two-step mechanism proposed in eq 3 since that mechanism (the first step is in rapid equilibrium and the observed radiolabel bound originates exclusively from the RQ′ complex) predicts a single exponential with an observed rate constant equal to k_{-1}. The fact that the observed rate constants for dissociation were essentially constant for both kinetic phases over the range of atropine con-

centrations tested (and when oxotremorine and unlabeled QNB were used as competing ligands) argues for the occurrence of two parallel dissociation reactions. The possibility that these two reactions are due to the two different classes of mAcChR observed in agonist titrations (see below) can be discounted since for all agonists tested the fraction of high- and low-affinity sites was essentially constant for several different membrane preparations, while the relative amplitudes of the two kinetic phases was dependent on the concentration of competing ligand. One possible explanation for the dissociation kinetics is that at high concentrations the competing ligand alters the state of the membrane-bound receptor, creating a second population of mAcChR-[^{3}H]QNB complexes that dissociates with a slower rate. This effect must be rapid compared to QNB dissociation since the distribution of [^{3}H]QNB-mAcChR into slowly and rapidly dissociating complexes must occur prior to [^{3}H]QNB dissociation. This could occur either by binding to a second site (having an affinity too low to be detected by Scatchard plots) on the protein or by altering the properties of the membrane. The latter possibility is not unreasonable since atropine, QNB, and oxotremorine are highly hydrophobic molecules. Thus, as the concentration of competing ligand is increased, the fraction of altered receptor molecules, decaying with $k_{obsd} \simeq 3 \times 10^{-5}$ s^{-1}, would increase concomitantly.

The values for K, k_1, and k_{-1} obtained in the above studies of [^{3}H]QNB association with porcine atrial membranes are in good agreement with a previous study on QNB interactions with the membrane-bound mAcChR from rat cerebral cortex and intestinal mucosa (Järv et al., 1979). However, those authors observed a single kinetic phase when measuring QNB dissociation: the observed rate constant was independent of competing ligand concentration. Thus, the biphasic decay observed in porcine atrial membrane-bound mAcChR may indicate either a difference in the properties of the mAcChR or, as suggested above, a difference in the ability of hydrophobic ligands to alter membrane structure in preparations from different sources.

Both antagonists and local anesthetics appeared to displace [^{3}H]QNB from the mAcChR in a competitive manner. The relative affinity for antagonists was in the order of QNB > 1-hyoscamine > atropine > scopolamine $\gg$ choline. The stereospecificity in antagonist binding was shown by the fact that 1-hyoscyamine (the active isomer) bound approximately threefold tighter than atropine (a racemic mixture of *d*- and *l*-hyoscyamine). In general (dibucaine was the exception), the potency of local anesthetics corresponded to their relative hydrophobicities with quinidine > tetracaine > lidocaine $\approx$ procainamide > dibucaine. Since quinidine, lidocaine, and procainamide are used clinically in the treatment of cardiac arrhythmias (Goodman & Gillman, 1975), one possible site of action in these compounds may be at cardiac mAcChR's (in addition to the well-known effects of local anesthetics on the potential-dependent sodium channel; Strichartz, 1973).

Agonist titrations of [^{3}H]QNB clearly deviated from results predicted for a homogeneous population of sites. Since Sharma & Banerjee (1978) have shown that ~40% of the QNB sites in rabbit heart preparations are presynaptic in origin, the simplest model consistent with agonist titrations was one in which there were two classes of noninteracting sites. Both pre- and postsynaptic mAcChR's would interact in an identical manner with QNB; however, they would differ in their relative affinities for agonists. By analogy with the studies in rabbit, the 20–35% of the mAcChR's in the high-affinity form for agonists are presynaptic while the remaining low-affinity sites would be postsynaptic in origin. At this time, however, this assumption must be considered speculative in nature, and clearly further evidence must be obtained. The relative affinities of agonists for the high-affinity sites were acetylcholine > oxotremorine > carbamylcholine > pilocarpine while the low-affinity sites showed an inversion of affinities with oxotremorine > acetylcholine > pilocarpine > carbamylcholine. These results were reproducible with several different preparations and may indicate a slightly different binding site topology for pre- and postsynaptic mAcChR's. A similar inversion of the order of affinity of ligands for high- and low-affinity mAcChR sites in rat brain preparations was observed by Birdsall et al. (1978). Their data showed that oxotremorine bound to the high-affinity site with approximately the same dissociation constant as acetylcholine, but oxotremorine bound 10-fold tighter than acetylcholine to the weak site. Furthermore, the relative affinities observed for the two sites (high to low affinity) varied from 250 for oxotremorine-M to 11 for (−)-acetyl-β-methylcholine. It is also of interest to note that the relative fraction of high-affinity sites observed by these authors (22–40%) was in the same range as that found in the above studies. α-Bungarotoxin (65 nm) did not show any affect on [^{3}H]QNB binding, indicating that none of the observed affects were mediated by nicotinic acetylcholine receptors.

In summary, this paper presents data characterizing the interaction of the membrane-bound mAcChR from porcine atria with agonists, antagonists, and local anesthetics. The simplest mechanism that appeared to be consistent with both the thermodynamic and kinetic data for [^{3}H]QNB binding to the mAcChR was one in which the initial ligand binding step was in rapid equilibrium, followed by a slow ligand-induced conformational change. The kinetic behavior observed for [^{3}H]QNB dissociation, however, may indicate that a more complex mechanism may be needed to completely explain all of the above data. The availability of large quantities of material from porcine atria, in addition to the similarity between porcine heart and the human heart, indicates that this may be a useful system for future studies of cardiac mAcChR's.

Acknowledgments

The authors acknowledge Paula Sparks for her expert typing and patience.

Appendix

Agonist titrations were fit by assuming one homogeneous population of sites for QNB that shows two noninterconvertible subpopulations of sites with respect to agonist interactions. Thus

$$[R_0] = [R_1]_0 + [R_2]_0 \tag{A1}$$

where $[R_0]$ is the total concentration of QNB sites and $[R_1]_0$ and $[R_2]_0$ are the two noninterconvertible classes of agonist binding sites. For QNB

$$K = \frac{[R_1][Q]}{[R_1Q]} = \frac{[R_2][Q]}{[R_2Q]} \tag{A2}$$

while for agonists (I)

$$K_1 = \frac{[R_1][I]}{[R_1I]} \qquad K_2 = \frac{[R_2][I]}{[R_2I]} \tag{A3}$$

The concentration of total receptor sites of class 1 is $[R_1]_0 = [R_1] + [R_1Q] + [R_1I]$. The fractional saturation of site 1 can then be calculated from the law of mass action:

$$\frac{[R_1Q]}{[R_0]} = \frac{([Q]/K)([R_1]_0/[R_0])}{1 + [I]/K_1 + [Q]/K} \quad (A4)$$

where [I] and [Q] are the concentrations of free agonist (agonist did not displace QNB at $[I]_0 \leq 10$[QNB sites]; thus, the free agonist concentration could be set equal to the total agonist concentration) and [^{3}H]QNB, respectively. Similarly, for site 2

$$\frac{[R_2Q]}{[R_0]} = \frac{([Q]/K)([R_2]_0/[R_0])}{1 + [I]/K_2 + [Q]/K}$$

Therefore

$$\bar{Y} = \frac{[R_1Q] + [R_2Q]}{[R_0]} = \frac{[Q]}{K}\left(\frac{F_1}{1 + [I]/K_1 + [Q]/K} + \frac{F_2}{1 + [I]/K_2 + [Q]/K}\right) \quad (A5)$$

where $F_1 = [R_1]_0/[R_0]$ and $F_2 = [R_2]_0/[R_0]$. The fractional saturation of QNB sites in the absence of agonist is $\bar{Y}_0$:

$$\bar{Y}_0 = [Q]/(K + [Q]) \quad (A6)$$

Since specifically bound [^{3}H]QNB and free [^{3}H]QNB were experimentally determined at each inhibitor concentration and K is known, the normalized binding isotherm

$$\% \text{ specifically bound} = \frac{\bar{Y}}{\bar{Y}_0} \times 100 \quad (A7)$$

could be calculated by using an iterative method where K_1, K_2, F_1, and F_2 were varied until the best fit was obtained. In general, fits to eq A5–A7 were sensitive to a 30% variation in K_1 and K_2 and a 5–10% variation in F_1 and F_2.

References

Best-Belpomme, M., & Dessen, P. (1973) *Biochimie 55*, 11–16.

Bevington, P. R. (1969) *Data Reduction and Error Analysis for the Physical Sciences* (particularly Chapters 4 and 9) McGraw-Hill, New York.

Birdsall, N. J. M., & Hulme, E. C. (1976) *J. Neurochem. 27*, 7–16.

Birdsall, N. J. M., Burgen, A. S. V., & Hulme, E. C. (1978) *Mol. Pharmacol. 14*, 723–736.

Bonner, R., Barrantes, F. J., & Jovin, T. (1976) *Nature (London) 263*, 429–431.

Burgermeister, W., Klein, W. L., Nirenberg, M., & Witcop, B. (1978) *Mol. Pharmacol. 14*, 751–767.

Cavey, D., Vincent, J. P., & Lazdunski, M. (1977) *FEBS Lett. 84*, 110–114.

Clark, D. G., Macmurchie, D., Elliot, E., Wolcott, R. G., Landel, A. M., & Raftery, M. A. (1972) *Biochemistry 11*, 1663–1668.

Detwiler, D. K. (1966) in *Swine in Biomedical Research* (Bustad, L. K., McClellan, R. O., & Burns, M. P., Eds.) pp 301–306, Frayn Printing Co., Seattle, WA.

Fields, J. Z., Roeske, W. R., Morkin, E., & Yamamura, H. I. (1978) *J. Biol. Chem. 253*, 3251–3258.

Galper, J. B., Klein, W. L., & Catterall, W. A. (1977) *J. Biol. Chem. 252*, 8692–8696.

Goodman, L. S., & Gillman, A. (1975) in *The Pharmacological Basis of Therapeutics*, pp 700–702, Macmillan, New York.

Hammes, G. G., & Wu, C. W. (1974) *Annu. Rev. Biophys. Bioeng. 3*, 1–33.

Hulme, E. C., Birdsall, N. J. M., Burgen, A. S. V., & Mehta, P. (1978) *Mol. Pharmacol. 14*, 737–750.

Janin, J. (1973) *Prog. Biophys. Mol. Biol. 27*, 77–120.

Järv, J., Hedlund, B., & Bartfai, T. (1979) *J. Biol. Chem. 254*, 5595–5598.

Lowry, O. H., Rosebrough, N. J., Farr, A. L., & Randall, R. J. (1951) *J. Biol. Chem. 193*, 265–275.

Quast, U., Engel, J., Heumann, H., Krause, G., & Steffen, E. (1974) *Biochemistry 13*, 2512–2520.

Scatchard, G. (1949) *Ann. N.Y. Acad. Sci. 51*, 660–672.

Sharma, U. K., & Banerjee, S. P. (1978) *Nature (London) 272*, 276–278.

Strange, P. G., Birdsall, N. J. M., & Burgen, A. S. V. (1978) *Biochem. J. 172*, 495–501.

Strichartz, G. R. (1973) *J. Gen. Physiol. 62*, 37–57.

Yamamura, H. I., & Snyder, S. H. (1974) *Proc. Natl. Acad. Sci. U.S.A. 71*, 1725–1729.